The CADEx Experiment: A new haloscope axion search in the 330-460 micro-eV mass range at the Canfranc Underground Laboratory (LSC)

Beatriz Aja,[a] **Sergio Arguedas Cuendis,**[b] **Eduardo Artal,**[a] **R. Belén Barreiro,**[c] **Francisco J. Casas,**[c] **Marina Calero de Ory,**[d] **Laura Castelló Gomar,**[c] **Alejandro Díaz-Morcillo,**[e] **Luísa de la Fuente,**[a] **Juan Daniel Gallego,**[f] **Benito Gimeno,**[g] **Alicia Gómez,**[d] **Daniel Granados,**[h] **Bradley J. Kavanagh,**[c] **María T. Magaz,**[d] **Jesús Martín-Pintado,**[d] **Enrique Martínez-González,**[c] **Jordi Miralda-Escudé,**[i,j,*] **Juan Monzó-Cabrera,**[e] **Francisco Najarro de la Parra,**[d] **José R. Navarro-Madrid,**[e] **Juan Pablo Pascual,**[a] **Alejandro Pascual Laguna,**[d] **Jorge Pelegrín,**[k] **Carlos Peña Garay,**[k] **José Reina-Valero,**[g] **David Rodríguez,**[d] **Víctor Rollano,**[d] **Fernando Teberio,**[l] **Jorge Teniente,**[m] **Patricio Vielva,**[c] **Iván Vila,**[c] **Rocío Vilar**[c] **and Enrique Villa**[a]

[a]*Departamento de Ingeniería de Comunicaciones, Univ. de Cantabria, 39005 Santander, Spain*

[b]*Consejo Nacional de Rectores (CONARE), San Jose, Costa Rica*

[c]*Instituto de Física de Cantabria (IFCA), CSIC-UC, 39005 Santander, Spain*

[d]*Centro de Astrobiología (CAB), CSIC-INTA, 28850 Torrejón de Ardoz, Madrid, Spain*

[e]*Dept. de Tecnologías de la Información y las Comunicaciones. Univ. Politécnica de Cartagena, 30302 Cartagena, Spain*

[f]*Centro Astronómico de Yebes, CDT, Instituto Geográfico Nacional (IGN), Guadalajara 19080, Spain*

[g]*Instituto de Física Corpuscular (IFIC), CSIC-University of Valencia, 46980 Valencia, Spain*

[h]*IMDEA Nanociencia, 28049 Madrid, Spain*

[i]*Institut de Ciències del Cosmos, Univ. de Barcelona, 08028 Barcelona, Spain*

[j]*Institució Catalana de Recerca i Estudis Avançats, 08010 Barcelona, Spain*

[k]*Laboratorio Subterráneo de Canfranc, 22880 Canfranc-Estación, Spain*

[l]*Anteral S.L., Polígono Areta, Badostain 2, 2º, 31620 Huarte, Navarra, Spain*

[m]*Institute of Smart Cities and Dept. of Electrical, Electronic and Communications Engineering, Public University of Navarra, 31006 Pamplona, Navarra, Spain*

The Canfranc Axion Detection Experiment (CADEx) will search for dark matter axions in the W-band (80–110 GHz) using a multiple cavity haloscope and highly sensitive Kinetic Inductance Detectors. A summary of the experiment and progress towards its construction is presented.

---

*Speaker

1. Introduction

The QCD axion model [1, 2] is the clearest solution to the strong CP problem of particle physics (or absence of parity violation in the strong interactions, and therefore of any neutron electric dipole), and at the same time predicts a perfect candidate to explain the Cold Dark Matter [3, 4] that is detected in cosmological observations and accounts for $\sim 5/6$ of all matter in the Universe [5, 6]. This has encouraged the experimental search of the axion using the inverse Primakoff effect, where photons created from the dark matter axions in a resonant cavity placed in a magnetic field are searched for by scanning over frequency corresponding to the unknown axion mass, $h\nu = m_a c^2$ [7]. So far, these experiments have mostly focused on frequencies below ~ 10 GHz owing to the increasing experimental difficulty with increasing frequency to reach a sufficient signal-to-noise for probing the expected axion-photon coupling constant $g_{a\gamma}$ (for a review, see, e.g., [8]). However, theoretical predictions suggest that the axion mass may well lie at higher frequencies (e.g. [9, 10]), depending on the uncertain prediction of the dark matter density in axions created in the early Universe, which depends on the complex physics of cosmological defects produced by the evolution of the axion field.

In this context, we are developing the Canfranc Axion Detection Experiment (CADEx), designed to operate over the frequency range 80 to 110 GHz or axion mass range 330 to 460 μeV, using the haloscope technique and exploring the use of Kinetic Inductance Detectors (KIDs) as broadband incoherent detectors, together with large axis ratio resonant haloscopes. CADEx also searches for other Beyond-the-Standard-Model particles, in particular Dark Photons, in a mass range where constraints from cosmology and astrophysics are weak, from the same data used for the axion search and any data taken without a magnetic field. At present, we expect to carry out a pathfinder phase in a dilution mK cryostat at the Instituto de Física de Cantabria (IFCA), with an initial phase without magnet to demonstrate the sensitivity for the dark photon search, and a second phase with a magnet for an initial axion search. The full CADEX experiment will then be installed in the cryostat facility at the Laboratorio Subterráneo de Canfranc (LSC), with improved instrumentation and the additional advantage of the shielding of cosmic radiation.

2. Conceptual design

CADEx was presented in our Collaboration paper [11], where the advantages of using coherent or incoherent detection are discussed in detail. Our main interest is in the use of incoherent detectors, with the initial plan to use Kinetic Inductance Detectors (KIDs), although other photon-counting technologies may be explored in the future. These detectors are characterized by the Noise Equivalent Power (NEP), which gives the noise N in the received power measured over a time interval Δt as $N = \text{NEP}/\sqrt{2\Delta t}$. At present, the KIDs technology already provides a signal-to-noise ratio similar to heterodyne detectors with a NEP of $\sim 3 \times 10^{-19}\,\text{W}/\sqrt{\text{Hz}}$ [12], but their future potential promises to reach values of NEP $\sim 10^{-20}\,\text{W}/\sqrt{\text{Hz}}$ [13].

A block diagram of CADEx is shown in Figure 1. The haloscope, thermally coupled to the mK stage, is in a magnetic field of $\sim 10\,\text{T}$, and its radiation is focused with horns and mirrors on the detector. The whole system is calibrated with an injected polarized signal of known intensity.
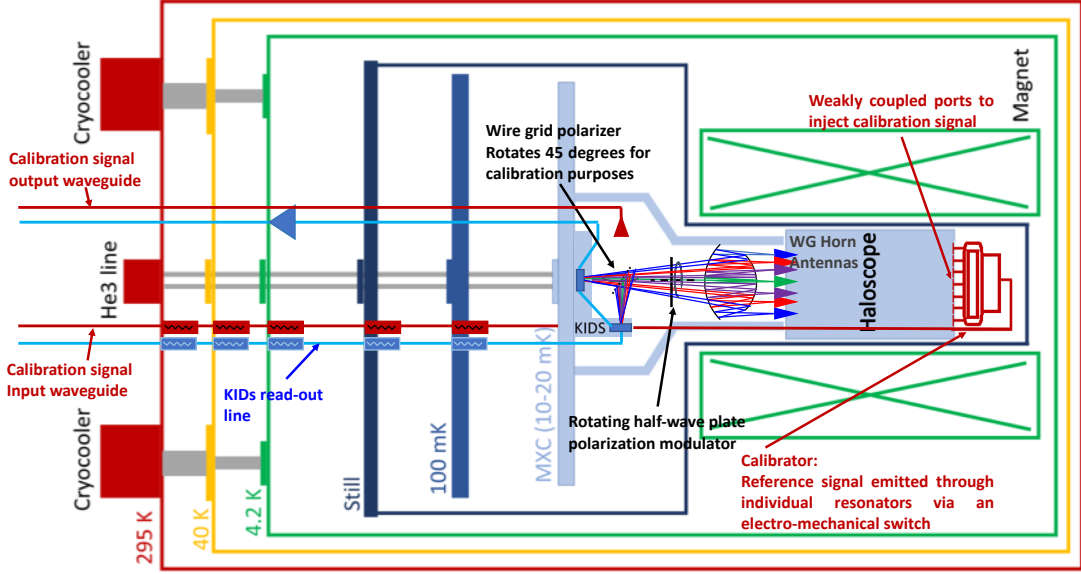
Figure 1: Schematic block diagram for CADEx. Colored boxes indicate temperature stages in the cryostat (red: ambient; yellow: 40 K; green: 4.2 K; light blue: 10–20 mK). Green boxes with diagonals depict the 10 T magnet operating at 4 K. The main CADEx subsystems in the mK stage are the haloscope (light blue inside the magnet), optics (7 coloured horns and rays), and two KID arrays to measure two orthogonal linear polarizations (dark blue). An externally injected calibration signal is shown in red.

Although the incoherent KID detectors are broadband receivers that do not resolve the narrow frequency spectral line generated by axions in the haloscope, any thermal radiation from the haloscope at $\nu \sim 100\,\text{GHz}$ is completely negligible even at $T = 0.1\,\text{K}$, so the important noise source is the detector noise, which does not depend on resolution, as well as radiation leaks into the cryostat. The CADEx detectors can distinguish a linearly polarized haloscope signal against the unpolarized background or other noise sources as a function of frequency as the haloscope is tuned, by switching polarization with a half-wave plate to mitigate fluctuations in the system gain and background in the final sensitivity [14]. Note that any signal coming from the haloscope, whether or not originating from axions, is polarized by design of the emitting horns, but as mentioned above the expected limitation of our sensitivity is not from any haloscope emission but from detector noise and background radiation external to the haloscope. The installation of CADEx at Canfranc will minimize the impact of cosmic rays on the detectors.

In the following sections, some of the progress in the experiment since our original publication [11], in relation to the haloscope and the KID detectors, is presented.

3. Haloscope construction and testing

The scaling of haloscope volume as the inverse cube of the search frequency is a challenge for axion searches at high frequency. We address this by designing a system of multiple rectangular

cavities with a large ratio of cavity length and height to width. The cavity width is then near 1.5 mm for 100 GHz. The ratio of length and height to width is limited, apart from the magnet bore volume, by the clustering of unwanted modes around the only mode of interest for axion detection, the TM_{110} in our solenoid magnet. This limit is more strict owing to mode crossings as the frequency is tuned. We find the maximum ratio of length and height to width to be around 50. In our present design, the signals from 7 cavities are coherently combined to a beam that is directed to the detector by our optical system. Each cavity comes with its horn, a mechanism to adjust the coupling based on a screw which is inserted into the waveguide port, and a tuning system based on a sliding wall that modifies the cavity width, with design specifications to keep the phase coherence and optimal coupling of the multiple cavities as the frequency is tuned.


| (a) | (b) |
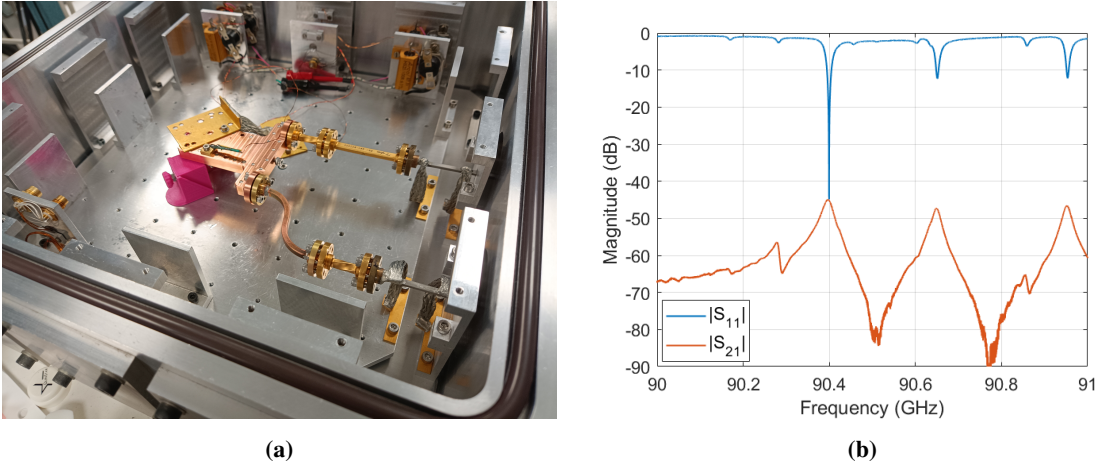
Figure 2: (a) Image of the haloscope placed inside the cryostat for characterization at cryogenic temperature. (b) Magnitude of the S-parameters measured from the cavity at $T = 11\,K$ and with the coupling screw inserted.

As an example of the progress made on the haloscope, Figure 2a shows the cavity connected to the waveguide ports placed in the cryostat for cryogenic characterization. The right plot (Figure 2b) depicts the measured S-parameters of the cavity, showing the first resonances. For testing purposes, these measurements were taken at $T = 11$ K, with the coupling screw inserted inside the waveguide by a fixed length. A comparison with electromagnetic simulations indicated that the resonance at 90.40 GHz is the axion mode (TM_{110}), with a coupling value near the optimal $\beta \sim 1$. The coupling screw in these measurements could not yet be moved, which is of vital importance during tuning. A cryogenic motor has recently been acquired to move the mechanical system and obtain the desired coupling at each frequency.

4. Detection System: Kinetic Inductance Detectors

The planned CADEx detection system is based on lumped-element KIDs (LEKIDs), where the superconducting inductor in the resonator will absorb the incident radiation modifying its kinetic inductance and resistance, lowering its resonant frequency and quality factor. KIDs developed for astronomical instrumentation have demonstrated state-of-the-art sensitivity at millimeter wavelengths [14, 15]. These KIDs are based on aluminum which has a low cut-off frequency for the

4

absorbed radiation of ~90 GHz, twice the superconducting gap [16]. CADEx is intended to cover the whole W-band (75 GHz to 110 GHz), which cannot be achieved with aluminum only KIDs. Extending the KIDs response below the Al cut-off frequency requires using superconductors with lower critical temperatures. We have explored the Titanium (Ti)/Aluminium (Al) bi-layer approach, which has demonstrated responsivity down to ~80 GHz [17].
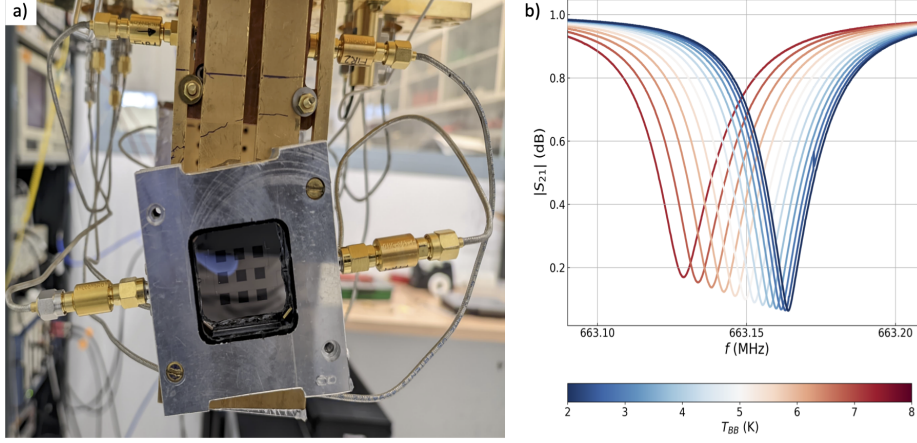
Figure 3: a) Image of the 3x3 LEKID array demonstrator integrated with a single read-out line (SMA horizontal connectors) installed in the mK stage of the CAB cryostat looking at the black body source for its characterization. **b)** Microwave transmission amplitude of one LEKID (resonator) as a function of the read-out frequency for different radiation powers coded with different colors indicated by the lower horizontal color scale bar. Vertical scale for the amplitude has been has been normalized to the out-of-resonance transmission. Note the shift of the resonant frequency towards lower values and the decrease of the quality factor as the absorbed power increases

We have designed and fabricated a 3-by-3 array of KIDs integrated with a single read-out line (Figure 3a). The array has been fabricated using a Titanium/Aluminum (Ti/Al) bilayer, where each layer is 15 nm thick. This bilayer exhibits a superconducting gap (Δ_0) of 112 μeV, allowing to decrease the KID's cut-off frequency to ~57 GHz. The KID optical design is optimized to cover the whole W-band [18].

Another key parameter for CADEx is the sensitivity of the detection system. We have characterized the response and sensitivity of the KID array in the mK dilution refrigerator of the Centro de Astrobiología (CAB, CSIC-INTA) equipped with a temperature-controlled black body radiation calibration source (Fig. 3a). A low-pass filter is placed in the optical path between the detectors and the black body to block radiation above 110 GHz. Fig. 3b displays the response of the resonator to the W-band radiation from the blackbody at temperatures ranging from 2.0 K to 8.0 K. The measured NEP reaches values of $\sim 5 \times 10^{-19}$ W Hz$^{-1/2}$ at 1 Hz, still above the baseline sensitivity requirement of CADEx, but with good perspectives to improve this by reducing the Two-Level System noise (see e.g. [19]) and optimizing the bilayer by changing the thickness of the Al and Ti layers. The quoted NEP has to be taken with caution since Ti compounds such as TiN show anomalous behavior, with a decreasing trend in NEP with increasing absorbed power [20]. Further measurements at lower power will be performed to confirm the behavior of the NEP with absorbed power. Additionally, we will implement strategies to alleviate the Two-Level System noise that

currently limits the sensitivity.

5. Projected Sensitivity

The left panel of Fig. 4 shows the projected 5σ sensitivity of CADEx to the axion-photon coupling $g_{a\gamma}$[1], assuming 7 cavities for a total haloscope volume $V = 0.08$ L; a magnetic field strength $B = 10$ T; an unloaded quality factor $Q_0 = 2 \times 10^4$; and a coupling factor $\beta = 1$. The vertical dashed black line corresponds to a three-month search centred on the axion mass of $m_a \sim 370\,\mu$eV ($f \sim 89.5$ GHz) and detector noise NEP $= 1 \times 10^{-19}$ W$/\sqrt{\text{Hz}}$ (the baseline noise target for the experiment). The region bounded by the solid black line can be explored by tuning the resonant frequency of the cavity. Given a cavity bandwith of $\Delta\nu_c = \nu_c/Q_\ell \approx 9$ MHz, the region between 80–110 GHz (corresponding to axion masses 330–460 μeV) could be covered with ~ 3000 exposures. Assuming future improvements in the NEP down to NEP $= 1 \times 10^{-20}$ W$/\sqrt{\text{Hz}}$, this would correspond to a measuring time of around 8 years (performing ~ 1 scan per day). The proposed set up should be able to probe down to axion-photon couplings of $g_{a\gamma} \approx 6 \times 10^{-13}$ GeV^{-1}, beginning to explore relevant parameter space for the QCD axion over mass range which is as-yet poorly explored.

The right panel of Fig. 4 shows the sensitivity to the kinetic mixing χ of Dark Photon DM, using the same data obtained for axions or data without a magnetic field. The sensitivity to χ, obtained from the axion-photon sensitivity by mapping $g_{a\gamma} \to \chi m_{\gamma'}/(\sqrt{3}B)$ (assuming random dark photon polarization [24]), reaches down to $\chi \sim 2 \times 10^{-14}$ in the CADEx frequency range. This is a significant improvement in this region of parameter space, where the overlap between experimental constraints [24, 25] and stellar cooling constraints [24] is weakest.

In summary, the Canfranc Axion Detection Experiment (CADEx) aims to the well-motivated parameter space of the QCD axion in the mass range $m_a \sim 370\,\mu$eV ($f \sim 89.5$ GHz) which is as-yet unexplored by haloscope experiments. Following an initial pathfinder phase installed at the Instituto de Física de Cantabria (IFCA), the full CADEx experiment will then be installed in the cryostat facility at the Laboratorio Subterráneo de Canfranc (LSC), with improved instrumentation and the additional advantage of the shielding of cosmic radiation. With this setup, CADEx will provide a sensitivity three orders of magnitude better than the current best broadband limit from the CAST helioscope [27], reaching the well-motivated region for QCD axion dark matter predicted from models [28–30]. Without additional data-taking, CADEx will also provide sensitivity to Dark Photon DM. CADEx will provide a multidisciplinary platform to develop novel concepts of haloscopes, including tunable-cavity haloscopes, and push the W-band superconducting detectors to their ultimate sensitivities.

---

[1]Full details of the sensitivity calculation can be found in e.g. Refs. [21–23].
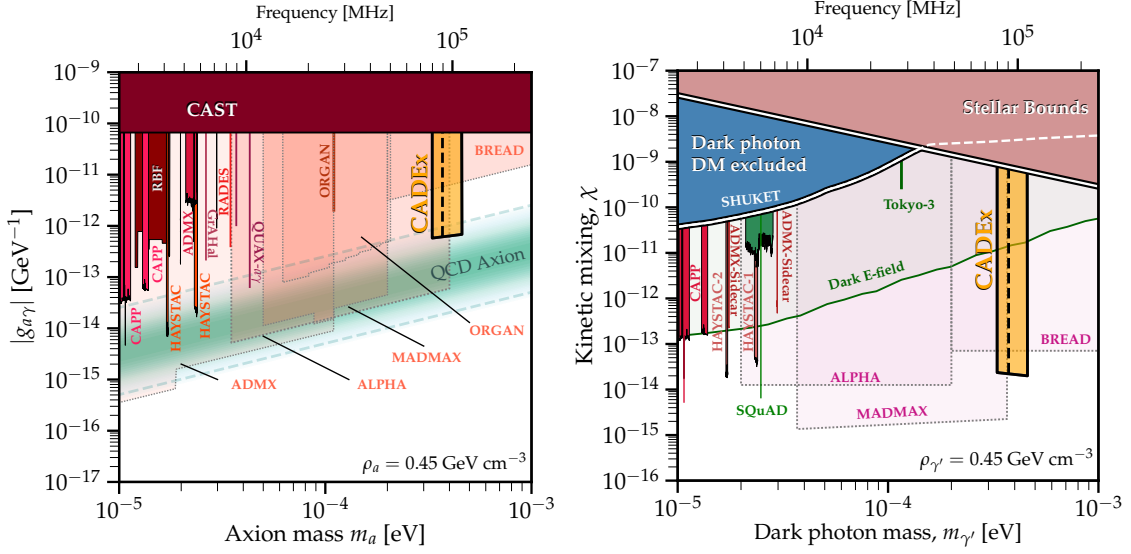
Figure 4: Projected CADEx sensitivity to the axion-photon coupling $g_{a\gamma}$ (left) and the dark photon kinetic mixing χ (right). The vertical black dashed line corresponds to a 3 month exposure at a single frequency with NEP of 10^{-19} W Hz$^{-1/2}$, while the yellow region covering 3000 frequency channels can be explored with a 10 times lower NEP over ~ 8 years. The left panel shows various constraints from axion haloscopes (filled red and purple regions), and projected constraints from future haloscopes (transparent red regions). In the right panel, the solid blue regions show where dark photons are excluded from being all of the Dark Matter on cosmological grounds [24, 25]. The brown region shows the envelope of constraints from stellar cooling (see [24] for a compilation). We show current and projected constraints from other axion haloscopes in red, with dedicated dark photon searches shown in green. Figures adapted from [26] and [24]. See Ref. [26] for full references.

PoS(COSMICWISPers2024)039

References

[1] R. Peccei and H. Quinn, CP *conservation in the presence of pseudoparticles*, *Phys. Rev. Lett.* **38** (1977) 1440.

[2] R. Peccei and H. Quinn, *Constraints imposed by* CP *conservation in the presence of pseudoparticles*, *Phys. Rev. D* **16** (1977) 1791.

[3] F. Wilczek, *Problem of strong P and T invariance in the presence of instantons*, *Phys. Rev. Lett.* **40** (1978) 279.

[4] S. Weinberg, *A new light boson?*, *Phys. Rev. Lett.* **40** (1978) 223.

[5] G. Bertone, D. Hooper and J. Silk, *Particle dark matter: Evidence, candidates and constraints*, *Phys. Rept.* **405** (2005) 279 [hep-ph/0404175].

[6] PLANCK collaboration, *Planck 2018 results. VI. Cosmological parameters*, *Astron. Astrophys.* **641** (2020) A6 [1807.06209].

[7] P. Sikivie, *Experimental Tests of the Invisible Axion*, *Phys. Rev. Lett.* **51** (1983) 1415.

[8] I.G. Irastorza and J. Redondo, *New experimental approaches in the search for axion-like particles*, *Prog. Part. Nucl. Phys.* **102** (2018) 89 [1801.08127].

[9] K. Saikawa, J. Redondo, A. Vaquero and M. Kaltschmidt, *Spectrum of global string networks and the axion dark matter mass*, *JCAP* **10** (2024) 043 [2401.17253].

[10] J.N. Benabou, M. Buschmann, J.W. Foster and B.R. Safdi, *Axion mass prediction from adaptive mesh refinement cosmological lattice simulations*, 2412.08699.

[11] B. Aja, S. Arguedas Cuendis, I. Arregui, E. Artal, R. Belén Barreiro, F.J. Casas et al., *The Canfranc Axion Detection Experiment (CADEx): search for axions at 90 GHz with Kinetic Inductance Detectors*, **2022** (2022) 044 [2206.02980].

[12] P. De Visser et al., *Fluctuations in the electron system of a superconductor exposed to a photon flux*, *Nature communications* **5** (2014) 1.

[13] S. Hailey-Dunsheath et al., *Kinetic inductance detectors for the origins space telescope*, *Journal of Astronomical Telescopes, Instruments, and Systems* **7** (2021) 011015.

[14] Adam, R. et al., *The nika2 large-field-of-view millimetre continuum camera for the 30 m iram telescope*, *A&A* **609** (2018) A115.

[15] E. O'Connor, A. Shearer and K. O'Brien, *Energy-sensitive detectors for astronomy: Past, present and future*, *New Astronomy Reviews* **87** (2019) 101526.

[16] P.K. Day et al., *A broadband superconducting detector suitable for use in large arrays*, *Nature* **425** (2003) 817.

[17] A. Catalano, A. Bideaud, O. Bourrion, M. Calvo, A. Fasano, J. Goupy et al., *Sensitivity of lekid for space applications between 80 ghz and 600 ghz*, *Astronomy & Astrophysics* **641** (2020) A179.

[18] M.C. de Ory, V. Rollano, D. Rodriguez, M.T. Magaz, D. Granados and A. Gomez, *Low loss hybrid nb/au superconducting resonators for quantum circuit applications*, *arXiv preprint arXiv:2401.14764* (2024) .

[19] N. Foroozani, B. Sarabi, S. Moseley, T. Stevenson, E. Wollack, O. Noroozian et al., *Dual-resonator kinetic inductance detector for distinction between signal and 1/f frequency noise*, *Physical Review Applied* **21** (2024) 014009.

[20] J. Bueno, P. Coumou, G. Zheng, P. De Visser, T. Klapwijk, E. Driessen et al., *Anomalous response of superconducting titanium nitride resonators to terahertz radiation*, *Applied Physics Letters* **105** (2014) .

[21] A.A. Melcón et al., *Axion Searches with Microwave Filters: the RADES project*, *JCAP* **05** (2018) 040 [1803.01243].

[22] A. Álvarez Melcón et al., *Scalable haloscopes for axion dark matter detection in the 30μeV range with RADES*, *JHEP* **07** (2020) 084 [2002.07639].

[23] B. Aja et al., *The Canfranc Axion Detection Experiment (CADEx): search for axions at 90 GHz with Kinetic Inductance Detectors*, *JCAP* **11** (2022) 044 [2206.02980].

[24] A. Caputo et al., *Dark photon limits: A handbook*, *Phys. Rev. D* **104** (2021) 095029 [2105.04565].

[25] P. Arias et al., *WISPy Cold Dark Matter*, *JCAP* **06** (2012) 013 [1201.5902].

[26] C. O'Hare, "cajohare/axionlimits: Axionlimits." https://cajohare.github.io/AxionLimits/, July, 2020. 10.5281/zenodo.3932430.

[27] CAST Collaboration collaboration, *New upper limit on the axion-photon coupling with an extended cast run with a xe-based micromegas detector*, *Phys. Rev. Lett.* **133** (2024) 221005.

[28] L. Di Luzio, F. Mescia and E. Nardi, *Redefining the Axion Window*, *Phys. Rev. Lett.* **118** (2017) 031801 [1610.07593].

[29] L. Di Luzio, F. Mescia and E. Nardi, *Window for preferred axion models*, *Phys. Rev. D* **96** (2017) 075003 [1705.05370].

[30] P. Agrawal et al., *Experimental Targets for Photon Couplings of the QCD Axion*, *JHEP* **02** (2018) 006 [1709.06085].